Adaptive Free-Space Cell Shaping Using Spatially Coupled MMF in Indoor OWC

Xinda Yan(1), Yuzhe Wang(1), Jin Shi(2*), Eduward Tangdiongga(1)

(1) Electro-Optical Communication Systems, Eindhoven University of Technology, 5612 AZ Eindhoven, The Netherlands
(2) School of Information Engineering, Wuhan University of Technology, Wuhan 430070, China
*e-mail address: jinshi@whut.edu.cn

Abstract The Gaussian-shaped beam from the laser source is controlled by MMF with adjustable offset launch distances and controllable external perturbations, resulting in a uniform ROP across optical free-space cells. Data rate of 10 Gbps is experimentally demonstrated over 10-degree full angle coverage in OWC downlinks.

Introduction

Optical wireless communication (OWC) offers an attractive solution to resolve congestions in radio links [1]. Compared to radio frequency, a 40 dBi directivity gain is easily achievable in optical spectrum without the need for any active components. In particular, the 1500nm window is eye-safety, compatible with existing fibre-optic networks, and well-suited for high-speed wireless transmission [2]. Therefore, line-of-sight (LOS) enabled single device exclusive links have been extensively investigated in OWC, with a transmission rate of 112 Gbps per beam already achieved [3]. However, precise alignment is required, especially for mobile terminals, which can be a limitation in real scenarios. To mitigate this issue, optical beams with larger divergent angles are preferred to cover a certain area. Nevertheless, users would experience a significant variation in received optical powers (ROPs) depending on their position relative to the optical antennas, which is influenced by commercially available lasers with Gaussian-shaped beams [4]. To generate intensity distributions of beams other than Gaussian, various methods have been explored, including traditional refractive and diffractive techniques for transforming Gaussian-shaped beams into flat-top beams, as well as the superposition of spatial modes in few-mode fibers (FMFs). [5].

This paper presents a novel indoor OWC transmitter that addresses the issue of ROP variation experienced by mobile terminals within optical free-space cells. The proposed scheme is based on two principles. Firstly, it employs mode selective excitation of a multi-mode fiber (MMF) [6], wherein higher order modes (HOMs) are gradually excited as the offset launch distance (OLD) increases. This results in the energy of speckle patterns flowing from the core center to core edges of the MMF. Secondly, the transmitter utilizes the mode coupling effect [7], where iteratively optimized external perturbations imposed on the MMF adjust coupling coefficients among propagating modes to achieve higher ROPs in the region of interest (ROI). By utilizing these two principles, a comparable ROP can be achieved across the entire cell, which is similar to optical beam steering. Demonstrated at a 10 Gbps OWC downlink over 10 degrees for a transmission distance of 1.5 m, the proposed scheme introduces minimal insertion loss (0.6 dB at the transmitter side). With a larger OLD (resulting in 3.5 dB loss), the scheme can cover larger areas. The authors believe that the great beam shaping capability of this MMF-based scheme could enable multi-user access.

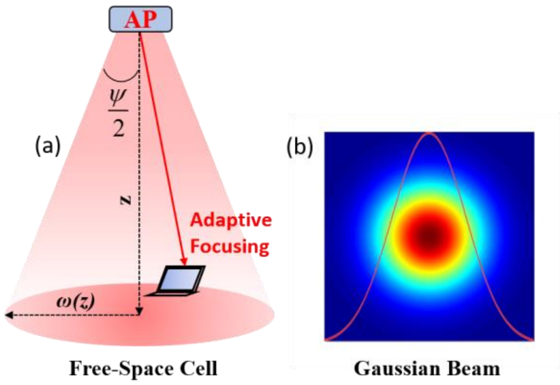

Fig. 1: Free-Space cell and Gaussian beam.

Principles

As shown in Fig. 1(a), a ceiling-mounted access point (AP) pointed towards the ground serves as an optical free-space cell. The beam is emitted by the AP with a full divergent angle $\psi=2*arctan(\omega(z)/z)$, where z is the wireless transmission distance, and $\omega(z)$ is the cell radius at the receiving plane. A laser beam with ideal Gaussian distribution can be characterized as: $I=I_0*exp(-2r^2/\omega^2(z))$, as illustrated in Fig.1 (b). I_0 is the peak intensity at the center of the beam, r is the radial distance away from the z axis, $\omega(z)$ is the $1/e^2$ radius when the intensity drops to 13.5% of I_0. We can simply infer that a user at the cell boundary would experience an approximately 8.7 dB ROP loss with respect to those at the cell center. To mitigate this ROP variation, MMF is introduced. Indeed, coherent beam coupled MMF results in speckle patterns at its distal end. Despite this, the scrambling effect of MMF is deterministic with a fixed configuration [8]. Moreover, MMF is sensitive to external perturbations, and it can achieve beam focusing without shaping the incident light [9]. By imposing controllable perturbations on MMF, its output speckle pattern approaches the target one in an iterative way. We define enhancement (*Eht*) in a certain ROI as: $Eht=P_{opt}/P_{avg}$. P_{opt} and P_{avg} are optimized and average ROP within a ROI, respectively. In this work, a fiber coupled collimator is served as the optical receiver. Therefore, the ROI equals to the clear aperture of the receiving collimator and the center of ROI is the location of the user. Since the intensity distribution of the averaged speckle patterns is Gaussian [10] and *Eht* is determined by the number of control units imposed on MMF, the optimized intensity distribution should also be Gaussian. Reviewing the Gaussian distribution of rapid decline as the radial distance increases, increasing P_{avg} at cell edges is the most effective way to homogenize the ROP variation. In this paper, a collimator pair is deployed to spatially couple the coherent laser beam into MMF as shown in Fig. 2.

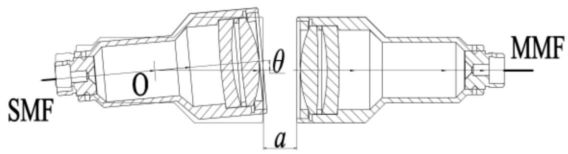

Fig. 2: Spatial coupling of MMF

A single mode fiber (SMF) with a Gaussian intensity distribution is connected to the front collimator. And the rear collimator is coupled into a 5m long OM1 standard MMF (∅=62.5μm). The coupling distance between the collimator pair is 12mm, and the front collimator is rotated around a fix point *O*. To quantize this angular offset, the collimator pair (F810FC-1550, Thorlabs) is simulated in Zemax. The mode field diameter (MFD) of the input fiber is set to be 9um, and it is characterized by an ideal Gaussian-shaped beam. Simulation results are shown in Fig. 3. The Coupling efficiency curve with different offset angle θ is shown in Fig. 3 (a). It is obvious that the rotation angle θ is dependent on the spatial coupling distance a, which is the distance between the collimator pair. Fig. 3 (b) shows a linear trend between the offset angle θ and OLD. Therefore, we can replace θ with an independent parameter, i.e., OLD. The coupling loss between SMF and MMF increases as a function of OLD.

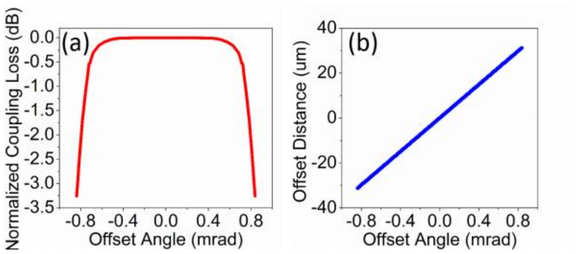

Fig. 3: Impact of offset angle in Zemax simulation

The coupling loss introduced by OLD is 0.1 dB when OLD equals to 22 μm, and rapid decline occurs from OLD = 27 μm to OLD = 31 μm. OLD = 31 μm corresponds to θ = 0.83 mrad, and the coupling loss at this point is 3 dB. Considering the OM1 MMF has a core radius of 31um, θ = 0.83 mrad is sufficient to fully excite HOMs of MMF at insertion loss of 3 dB. A θ larger than 0.83 mrad is not considered in our simulation since the peak intensity of the incident Gaussian-shaped beam would exceed the core area of MMF. Marked by coupling loss, the same state of mode excitation of MMF can be easily repeated in experiments. Since HOMs are gradually excited as OLD increases, OLD is expected to adjust the proportion of spatial modes. In this paper, the coupling loss introduced by OLD is selected as 0.1 dB to minimize the optical power loss. Besides, a 0.5 dB coupling loss is experimentally measured at the MMF output when the collimator pair is fully aligned. Therefore, a total coupling loss of 0.6 dB is expected in following experiments.

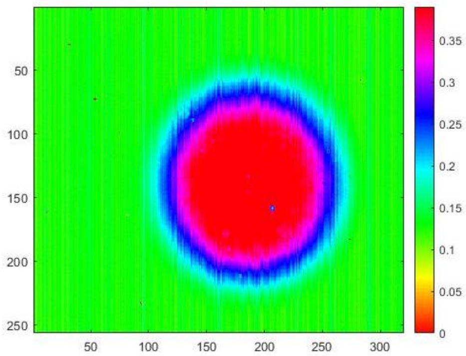

Fig. 4: Averaged Intensity distribution at 31 μm OLD

The averaged intensity distribution shown in Fig. 4. is measured by averaging 800 random speckle patterns at OLD = 31 μm. With a large OLD, the averaged intensity distribution of speckle patterns shows remarkable uniformity. Because sufficiently exited HOMs compensate ROP at beam outer ranges, the intensity at beam boundary is only 3 dB smaller than that at beam center. Therefore, the collimator pair can always optimize the ROP of mobile terminals by different OLD, regardless their position relative to the optical antennas.

Experimental Setup

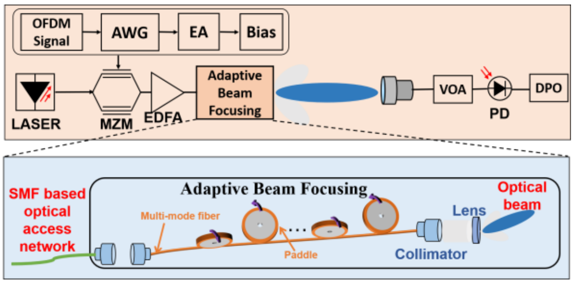

Fig. 5: Experimental setup of the OWC system with adaptive beam focusing.

The proposed experimental setup for OWC system with adaptive beam focusing or steering is illustrated in Fig. 5. In order to improve the spectral efficiency, an orthogonal frequency division multiplexing (OFDM) signal is generated offline, with a block size of fast Fourier transform (FFT) of 256. The cyclic prefix (CP) length and the modulation order of quadrature amplitude modulation (QAM) symbol are kept constant at 16. Subsequently, the OFDM signal is fed into an arbitrary waveform generator (AWG), which produces an analog electrical signal with a sampling rate of 5 GSa/s. This electrical signal is then amplified using an electrical amplifier (EA) to increase its power. The amplified signal is superimposed with direct current (DC) using a bias tee to ensure that the electrical signal works in the linear region of the Mach-Zehnder modulator (MZM). The laser used for the system operates at a wavelength of 1550 nm, which is compatible with the current single-mode fiber (SMF) based optical access network. The optical signal is boosted by an erbium-doped fiber amplifier (EDFA) to 10 mW. To enable beam steering for the OWC system, an adaptive beam focusing based transmitter is used to vary the transmitted angle of the optical beam. After transmitting through a 1.5-m free space, a collimator is placed before the photodiode (PD) to receive the optical signal. After optical-electric conversion, the electrical signal is converted into digital signals by a digital phosphor oscilloscope (DPO) for further digital signal processing.

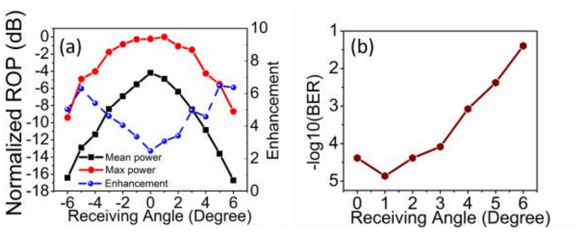

Fig. 6: (a) Normalized and enhancement ROP (b) BER performance versus receiving angles

To investigate the difference of ROP over the receiving plane, a SMF coupled collimator is placed at 1.5 m away from the optical transmitter, and ROP measurements are taken at 11 discrete target receiving positions. The target positions range from -5 degrees to +5 degrees with an interval of 1 degree, and it is achieved by longitudinally moving the receiving collimator along a rail. The mean values and maximum values of ROPs at different angles are measured, as shown in Fig. 6(a). When the receiving angle is 0 degrees, the mean ROP curve (marked in black) reaches its maximum. The descent speed of mean ROP increases as the receiving angle increases. As for the maximum ROP (marked in red), it remains basically consistent between negative 3-degree and positive 3-degree, with a decrease in ROP of no more than 2 dB. Compared to 3-degree, another 3 dB degradation of maximum ROP occur at 4-degree. When the receiving angle reaches 6-degree, the maximum ROP has decreased by more than 8 dB, although enhancement shows an upward trend as the angle increases. Since the BER performance depends on ROP in our system, BER curve with the same trend as ROP curve is shown in Fig. 6(b). The system can achieve a BER below 2.4×10^{-2} at 10Gbps over 10 degrees. Moreover, the same level of BER performance is maintained within 3 degrees. It is worth noting that the performance at opposite angles exhibits similar performance due to the circular symmetry of the averaged intensity distribution of speckle patterns. As a result, we can conclude that a 6-degree coverage area with high uniformity of BER performance is achieved in our proposed system, at the cost of 0.6 dB coupling loss (at transmitter). With the proposed cell shaping method enable by MMF, the mobility limitation of end-users is mitigated. As the OLD further increase (at the cost of higher loss), a constant enhancement is expected, and the coverage area of each AP can be extended.

Conclusions

In this paper, adaptive beam focusing is achieved by using an OM1 standard MMF and rotating polarization controllers. To further enable spatial modulation, a collimator pair is introduced, which adds an extra dimension to modulate the MMF at its distal end. With a measured coupling loss of 3.5 dB at the distal end of MMF, HOMs are sufficiently excited, resulting in a uniformly distributed ROP within the beam, and the optical free-space cell. This approach mitigates the mobility limitations of mobile users in a LOS OWC link. Additionally, the proposed collimator pair allows for continuous adjustment of the MMF's OLD with high repeatability. With a minimized spatial coupling loss of 0.6 dB, a 10 Gbps OWC downlink is able to cover a full angle range of 10 degrees, achieving a BER lower than 2.4×10^{-2}.

References

[1] K. Wang, S. Arnon, Z. Ghassemlooy, S. Zvanovec, W. Li, J. Elmirghani, "Evolution of Short-Range Optical Wireless Communications," Journal of Lightwave Technology, vol. 41, no. 4, pp. 1019-1040, 2023, DOI: 10.1109/JLT.2022.3215590.

[2] T. Koonen, K. Mekonnen, Z. Cao, F. Huijskens, N. Q. Pham, and E. Tangdiongga, “Ultra-high-capacity wireless communication by means of steered narrow optical beams,” Philos. Trans. R. Soc. Math. Phys. Eng. Sci., vol. 378, no. 2169, 2020, DOI: 10.1098/rsta.2019.0192.

[3] F. Gomez-Agis, S. P. van de Heide, C. M. Okonkwo, E. Tangdiongga and A. M. J. Koonen, "112 Gbit/s Transmission in a 2D Beam Steering AWG-Based Optical Wireless Communication System," 2017 European Conference on Optical Communication (ECOC), Gothenburg, Sweden, 2017, pp. 1-3, DOI: 10.1109/ECOC.2017.8346059.

[4] H. Al Hajjar, B. Fracasso, and K. Heggarty, "Uniform free-space cell shaping using diffractive-type beam diffusers for optical wireless links," Optics Letters, Vol. 39, no. 24, pp. 6871-6874, 2014, DOI: 10.1364/OL.39.006871.

[5] C. Xu, X. Liu, L. Zhang, Z. Xiao, and X. Feng, “All-fiber laser with flattop beam output using a few-mode fiber Bragg grating,” Optics Letters, vol. 43, no. 6, pp. 1247–1250, 2018, DOI: 10.1364/OL.43001247.

[6] H. Li, Y. Liu, H. Liang, S. Han and Z. Wang, "Twist-Related Speckle Variation in Graded-Index Multimode Fiber," in IEEE Photonics Journal, vol. 10, no. 5, pp. 1-9, 2018, DOI: 10.1109/JPHOT.2018.2868276.

[7] R. Olshansky, "Mode Coupling Effects in Graded-Index Optical Fibers," Appl. Opt. vol. 14, no. 4, pp. 935-945, 1975, DOI: 10.1364/AO.14.000935.

[8] D. Stellinga, S. Pradhan, M. P. van Exter, and P. Lodahl, “Time-of-flight 3D imaging through multimode optical fibers,” Science, vol. 374, no. 6573, pp. 1395-1399, 2021, DOI: 10.1126/science.abl3771.

[9] S. Resisi, Y.Viernik, Sebastien M. Popoff, Y. Bromberg, “Wavefront shaping in multimode fibers by transmission matrix engineering,” APL Photonics, Vol. 5, no. 3, pp. 1-7 (036103), DOI: 10.1063/1.5136334

[10] B. Zhang, S. A. Goorden, A. P. Mosk, and W. L. Vos, "A reference-defining criterion for light focusing through scattering media based on circular Gaussian distribution of speckle background intensity," Sci. Rep., vol. 8, no. 1, p. 6385, Apr. 2018, DOI: 10.1038/s41598-018-24698-0.